



Cite this: *Chem. Sci.*, 2021, **12**, 3202

All publication charges for this article have been paid for by the Royal Society of Chemistry

Received 22nd October 2020
 Accepted 2nd January 2021

DOI: 10.1039/d0sc05813k
rsc.li/chemical-science

Introduction

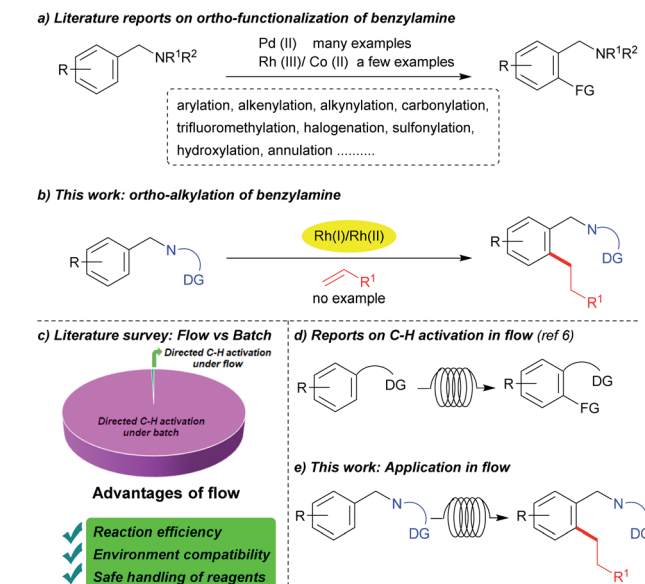
Benzylamine derivatives are important core structures in various biologically active compounds and natural products.¹ Hence, the functionalization of benzylamine derivatives *via* C–H bond activation strategies is one of the more important areas in organic chemistry.² Direct functionalization and a directing group strategy have both been used for this type of derivatization. The *ortho*-functionalization of benzylamine derivatives, such as carbonylation,^{2a} alkenylation,^{2b} alkylation by using alkyl halides,^{2c} trifluoromethylation,^{2d} halogenation,^{2e} arylation,^{2g} sulfonylation,^{2k} and hydroxylation^{2l} using Pd complexes as catalysts have been reported (Scheme 1a). Apart from the use of palladium, only a few examples of the use of other metals as catalysts, such as Co^{2h–j} or Rh^{2f} for annulation or alkynylation reactions with alkynes have been reported. Given our continuous interest in C–H alkylation reactions,³ we were strongly motivated to investigate the *ortho*-alkylation of benzylamines with alkenes as alkyl sources, which, as of this writing, does not appear to have been reported (Scheme 1b).

Flow chemistry is a growing field of research in organic chemistry. In industrial research, it is well known that flow chemistry has great advantages and is now a well-established process that has a variety of applications.⁴ In recent years flow transformation reactions have also found their way into academic research laboratories.⁵ Considering the advantages of flow chemistry over traditional batch reactions, such as reaction efficiency, safety, and environmental compatibility,^{5a–c} we evaluated the potential of this process for use in the reaction described in this report. Because flow chemistry has not been

extensively explored in the case of C–H bond activation (Scheme 1c),⁶ there is no apparent reason for why its flow conditions could not be used in this area of research (Scheme 1d). To our delight, we successfully optimized the conditions for our reaction even under flow. Moreover, the advantages of this process over batch reactions are also presented (Scheme 1e).

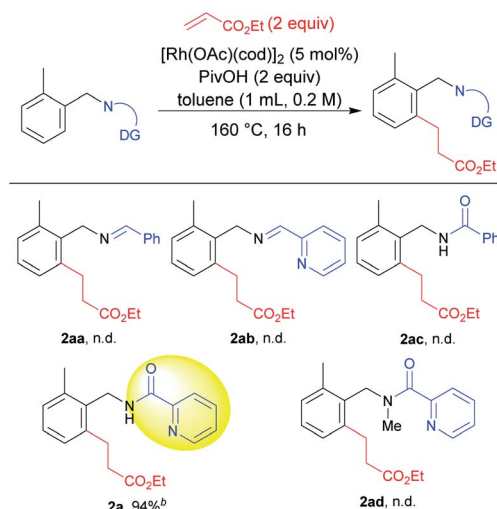
Results and discussion

We selected 2-methylbenzylamine and ethyl acrylate as model substrates to screen various directing groups⁷ using [Rh(OAc)(cod)]₂ as a catalyst and pivalic acid as an additive in toluene as a solvent at 160 °C for 16 h (Table 1). An imine



Scheme 1 Functionalization of benzylamine.



Table 1 Evaluation of directing groups^a

^a Reaction conditions: **1** (0.2 mmol), ethyl acrylate (0.4 mmol), $[\text{Rh}(\text{OAc})(\text{cod})]_2$ (0.01 mmol), PivOH (0.4 mmol), toluene (1.0 mL) at 160 °C for 16 h. ^b Determined by ^1H NMR analysis of the crude mixture. n.d. = not detected.

directing group failed to give the product **2aa**. We then hypothesized that a bidentate directing group might promote the reaction. However, the imine prepared from 2-pyridinecarboxaldehyde also failed to provide the desired product **2ab**. We next focused on the use of an amide directing group for this transformation. Our hypothesis was correct regarding the use of an amide directing group and the use of a picolinamide derivative promoted the reaction to a significant extent, with **2a** being produced in a high yield, whereas in the absence of a nitrogen atom in the directing group, **2ac** was not produced. Furthermore, to check the importance of a free NH moiety, we prepared a *N*-Me protected directing group. However, no **2ad** was formed when the *N*-Me protected directing group was used, which supports the fact that the presence of a free NH group on the bidentate coordination group is crucial for the reaction to proceed.

With a suitable directing group being identified, we proceeded to optimize the reaction conditions (Table 2). After screening a series of reaction temperatures, 160 °C was found to give a high yield of **2a** (Table 2, entries 1–3). The amount of acid additive used in the reaction was also screened. Comparing entries 3–5, it was found that the use of 2 equiv. of pivalic acid was needed to achieve optimal conditions for this reaction (entry 3). The amount of ethyl acrylate was also found to be important for achieving a high yield. When it was decreased to 1.2 equiv. from the standard amount of 2 equiv., a lower product yield was obtained (entry 6). We further examined some other Rh catalysts such as Rh(i) (entries 7 and 8), Rh(ii) (entry 9), and Rh(iii) (entry 10) as catalysts for this transformation. The Rh(ii) acetate dimer also provided the product in an excellent yield of 97% (entry 9). On the other hand, the Rh(iii) catalyst was completely unreactive (entry 10). Finally, by slightly increasing the reaction temperature to 170 °C and using the Rh(ii) acetate

Table 2 Optimization of C–H alkylation reaction of **1a**^a

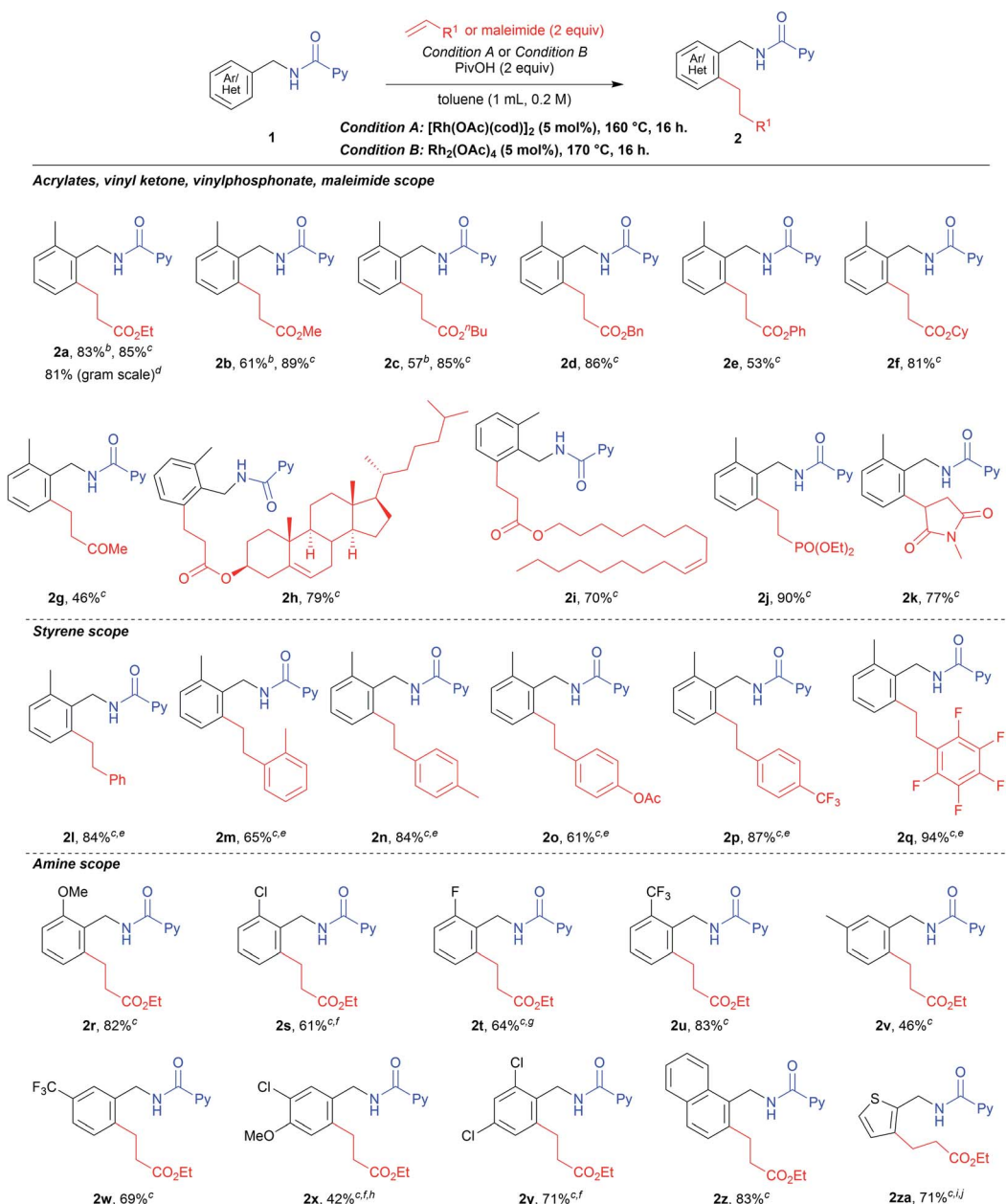
Entry	Catalyst	Temp.	Yield of 2a ^b (%)
1	$[\text{Rh}(\text{OAc})(\text{cod})]_2$	120 °C	2
2	$[\text{Rh}(\text{OAc})(\text{cod})]_2$	150 °C	26
3	$[\text{Rh}(\text{OAc})(\text{cod})]_2$	160 °C	94(83) ^c
4 ^d	$[\text{Rh}(\text{OAc})(\text{cod})]_2$	160 °C	10
5 ^e	$[\text{Rh}(\text{OAc})(\text{cod})]_2$	160 °C	62
6 ^f	$[\text{Rh}(\text{OAc})(\text{cod})]_2$	160 °C	27
7	$[\text{RhCl}(\text{cod})]_2$	160 °C	11
8	$[\text{RhCl}(\text{PPh}_3)_3]_2$	160 °C	58
9	$\text{Rh}_2(\text{OAc})_4$	160 °C	97
10	$[\text{Cp}^*\text{RhCl}_2]_2, \text{AgSbF}_6$ (20 mol%)	160 °C	n.d.
11	$\text{Rh}_2(\text{OAc})_4$	170 °C	99 (85) ^c

^a Reaction conditions: **1a** (0.2 mmol), ethyl acrylate (0.4 mmol), catalyst (0.01 mmol), PivOH (0.4 mmol), toluene (1.0 mL) at specified temperature for 16 h. ^b Determined by ^1H NMR analysis of the crude mixture. ^c Isolated yield. ^d No additive was used. ^e PivOH (1 equiv.) was used. ^f Ethyl acrylate (1.2 equiv.) was used. n.d. = not detected.

dimer, a quantitative yield of the desired product **2a** was observed (entry 11). From the catalyst screening data, we obtained an interesting finding in that both Rh(i) (entry 3) and Rh(ii) catalysts (entries 9 and 11) showed similar reactivities, giving high yields of the desired product. Finally, these conditions were determined to be the standard reaction conditions.

With the optimized conditions in hand, we next examined the substrate scope for the reaction (Table 3). The reaction of **1a** with ethyl acrylate gave **2a** in 83% isolated yield under the conditions shown in entry 3, Table 2. However, a lower isolated yield was obtained in the reaction with methyl acrylate (**2b**, 61%). By changing the reaction conditions to that used in entry 11, Table 2, the yield of **2b** was sharply increased to 89% isolated yield. From this result, we decided to use mainly condition B for further investigations into the substrate scope. Not only ethyl (**2a**) and methyl (**2b**) but also *n*-butyl (**2c**) and more sterically congested acrylates such as benzyl (**2d**), phenyl (**2e**) and cyclohexyl (**2f**) acrylates all gave the corresponding products in good to high yields. A simple methyl vinyl ketone also gave the desired product **2g** in moderate yield. With the successful identification of various acrylate coupling partners, we then examined C–H alkylation reactions with acrylates derived from biologically active compounds. When an acrylate derived from the essential animal sterol cholesterol was subjected to the alkylation reaction, the desired product **2h** was produced in 79% isolated yield. Another candidate for biologically useful compounds was synthesized from oleyl alcohol which is an unnatural fatty alcohol and the reaction showed a high tolerance (**2i**). When diethyl vinylphosphonate was used, the desired product **2j** was obtained in 90% yield. The maleimide derivative



Table 3 Substrate scope^a

^a Reaction conditions: **1** (0.2 mmol), α,β -unsaturated compound (0.4 mmol), catalyst (0.01 mmol), PivOH (0.4 mmol), toluene (1.0 mL) at the specified temperature for 16 h. Isolated yields are reported in all cases. ^b Condition A was used. ^c Condition B was used. ^d 1.32 g of **2a** was obtained from 5 mmol scale synthesis. ^e 7.5 mol% Rh₂(OAc)₄ and 5 equiv. styrene derivative were used. ^f A trace amount of the alkenylation product was observed. ^g 9% alkenylation product was observed. ^h A di-alkylation product was obtained in 28% yield. ⁱ 7.5 mol% of Rh₂(OAc)₄ was used. ^j An alkenylation product was obtained in 18% yield.

was also well tolerated under the reaction conditions to deliver the product **2k** in high yield. The scope of styrene derivatives was also examined, where an increased amount of the styrene substrate and 7.5 mol% of Rh₂(OAc)₄ were needed to produce high yields of the desired products (**2l**–**2q**). We then moved our focus to testing the effect of substituent groups on the benzylamine moiety. Benzylamine derivatives bearing both electron-donating (**2r**) and electron-withdrawing (**2s**–**2u**) groups

provided the expected products in high yields. To our delight, *meta*-substituted benzylamines resulted in a regioselective C–H alkylation to give the desired mono-alkylation products in moderate (**2v**) to high yields (**2w**). However, a starting material derived from 3-chloro-4-methoxybenzylamine resulted in the formation of the di-alkylation product in 28% yield, along with desired product **2x**, probably due to the smaller sized substitution at the *meta* position. A di-substituted benzylamine

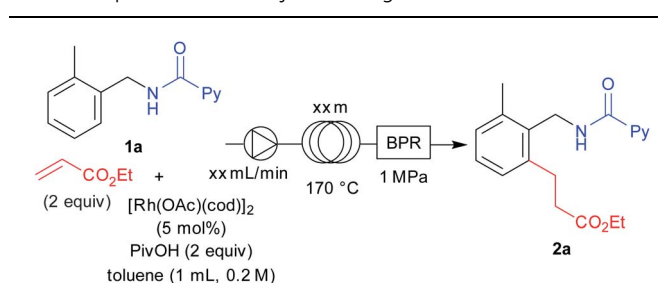


moiety was also suitable, with the corresponding product **2y** being produced in 71% yield. In the case of naphthylmethyl amine, the *ortho*-alkylation product **2z** was formed as the sole product in excellent yield. The thiophen-2-ylmethylamine derivative reacted smoothly to give **2za** in 71% yield, along with a minor amount of the alkenylated product. We also carried out the reaction on a gram scale to show practical utility of our catalytic system on a bulk scale and **2a** was produced in high yield.

We next turned our attention to optimizing the reaction conditions under a flow set up. A stock solution of the starting materials was prepared by dissolving **1a**, ethyl acrylate (2 equiv.), $[\text{Rh}(\text{OAc})(\text{cod})]_2$ (5 mol%), and PivOH (2 equiv.) in toluene (1 mL, 0.2 M). The solution was pumped using a dual pump at various flow rates and the solution was allowed to flow through a certain length of a stainless-steel loop that was immersed in an oil bath at 170 °C and further connected through a back-pressure regulator with a pressure of 1 MPa. After allowing 1 mL of the stock solution into the flow setup, an additional 15 mL of toluene was then allowed to flow after all of the stock solution had passed through the set-up, in order to collect the sample completely. We conducted a few optimizations for this set-up to obtain the optimal residence time for the flow reaction. It is noteworthy that we used $[\text{Rh}(\text{OAc})(\text{cod})]_2$ as the catalyst because it is soluble in the reaction solvent which is crucial, since the reaction mixture needed to be completely homogeneous before being pumped through the flow pump. After screening several conditions, we obtained an optimal residence time of 196 minutes by using a 10 meter loop at a flow rate of 0.04 mL min⁻¹ for this reaction towards full completion (Table 4, entry 3).

Having the optimized reaction under flow conditions in hand, we next examined the substrate scope under flow

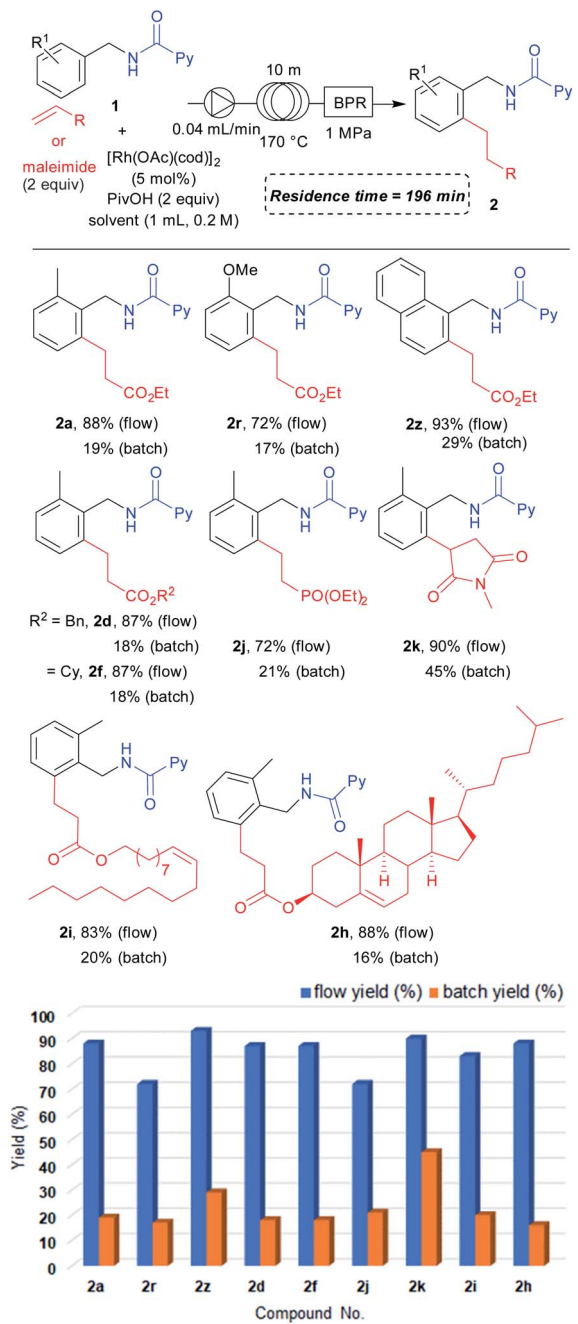
Table 4 Optimization and system design under flow^a



Entry	Loop length (xx m)	Flow rate (xx mL min ⁻¹)	Residence time (min)	Yield of 2a ^b (%)
1	5	0.05	79	30
2	10	0.05	157	80
3	10	0.04	196	88

^a Reaction conditions: a stock solution containing **1a** (0.2 mmol), ethyl acrylate (0.4 mmol), $[\text{Rh}(\text{OAc})(\text{cod})]_2$ (0.01 mmol) and PivOH (0.4 mmol) in toluene (1.0 mL) was prepared and the resulting solution was allowed to flow through the stainless loop at a specified flow rate. ^b Determined by ¹H NMR analysis of the crude mixture collected over three fractions to obtain the average value.

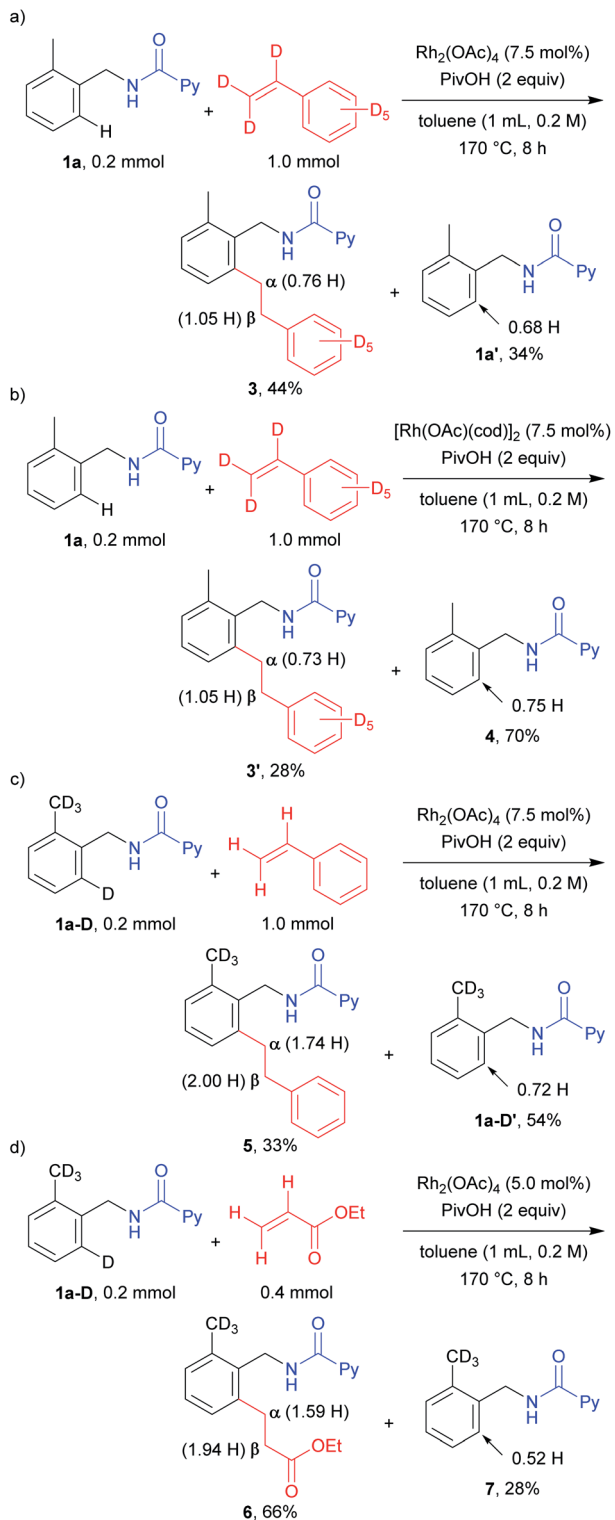
Table 5 Substrate applicability under flow^a



^a Reaction conditions for flow: **1** (0.2 mmol), α,β -unsaturated compound (0.4 mmol), $[\text{Rh}(\text{OAc})(\text{cod})]_2$ (0.01 mmol) and PivOH (0.4 mmol) were dissolved in toluene (1.0 mL) to prepare a stock solution which was then allowed to flow through the stainless loop at a rate of 0.04 mL min⁻¹. Determined by ¹H NMR analysis of the crude mixture collected over three fractions to obtain the average value. Reaction conditions for batch: **1** (0.2 mmol), α,β -unsaturated compound (0.4 mmol), $[\text{Rh}(\text{OAc})(\text{cod})]_2$ (0.01 mmol), PivOH (0.4 mmol), and toluene (1.0 mL) at 170 °C for 196 minutes. Determined by ¹H NMR analysis of the crude mixture.

conditions (Table 5). Both *ortho*-methyl- (**2a**) and methoxy-substituted (**2r**) benzylamine derivatives provided the desired products in excellent yields. The naphthylmethyl amine derived



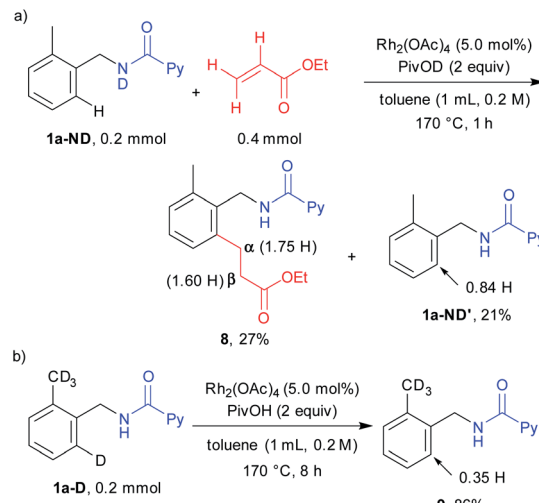


Scheme 2 Deuterium labelling experiments (1).

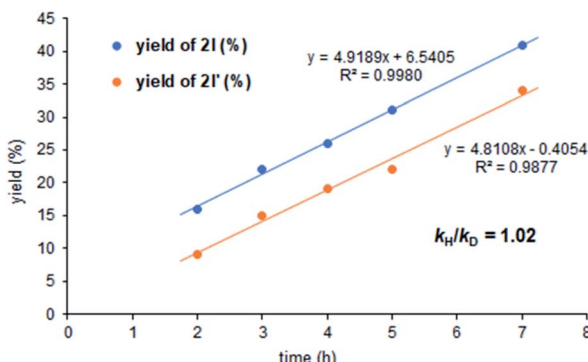
substrate also provided **2z** in an excellent yield. For the scope of alkenes, benzyl (**2d**), cyclohexyl (**2f**) acrylates and diethyl vinylphosphonate (**2j**) all furnished the desired products in high yields under flow conditions. We also obtained **2k** in excellent yield in the reaction with *N*-methylmaleimide. Biologically

active alcohol derived acrylates could also be used under the flow conditions to give high yields of **2i** and **2h**. We further conducted comparison reactions between flow and batch under similar reaction conditions (reaction time 196 minutes). To our delight, flow conditions provided the desired products in higher yields compared to batch reactions performed under a shorter reaction time. These data clearly show the advantages of flow conditions over batch reaction conditions in that the yield could be increased in only 196 minutes of reaction time. The reaction efficiency can be significantly improved by increasing the surface area to volume ratio in a flow process compared to that in a batch process which helps to distribute the heat transfer in the overall system more smoothly. This could be one of the explanations for the high efficiency of the reaction under flow conditions even when a shorter reaction time is used. However, this may not be the only reason for the significant improvement in reaction efficiency under flow conditions. Importantly, the reaction can be performed safely even when the reaction temperature is higher than the solvent's boiling point.

To investigate the mechanistic aspects of this C–H alkylation reaction, deuterium labelling experiments were carried out. When **1a** was treated with styrene-*d*₈ for a shorter reaction time in the presence of the Rh(*ii*) catalyst, 0.76 H was incorporated at the *α* position and 1.05 H at the *β* position in the product **3**, suggesting that the mechanism is not a simple one (Scheme 2a). In addition, the *ortho* C–H bond in the recovered starting material contained 0.32 D. This result clearly indicates that the cleavage of the *ortho* C–H and C–D bonds is reversible. To determine whether the mechanism is the same or different, depending on the oxidation state of the Rh complexes, we also performed the above reaction using [Rh(OAc)(cod)]₂ as the catalyst (Scheme 2b). A similar H/D scrambling was observed, where 0.73 H and 1.05 H were incorporated at the *α* position and the *β* position in **3'**, respectively. In addition, a deuterium atom was also incorporated (0.25 D) into the starting material. These results imply that both the Rh(*i*) and Rh(*ii*) catalytic systems appear to follow the same reaction mechanism. When



Scheme 3 Deuterium labelling experiments (2).

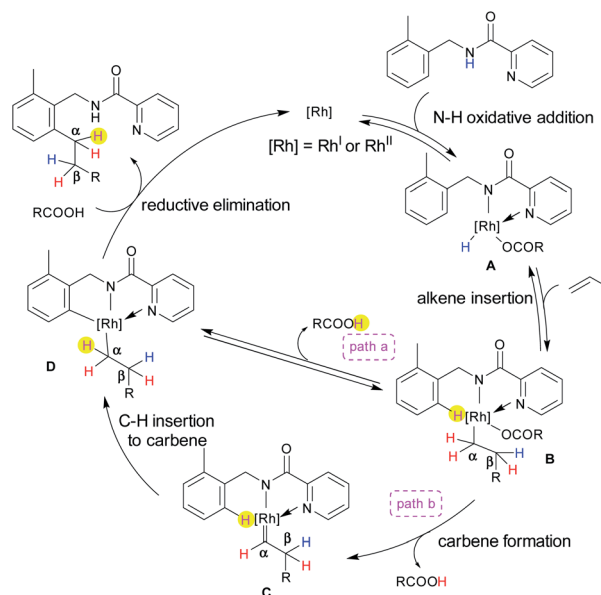
Fig. 1 Determination of the k_H/k_D ratio.

the isotopically labelled substrate **1a-D** was reacted with styrene, a 0.26 D incorporation was observed at the α position of the product **5** (Scheme 2c). On the other hand, no deuterium atom incorporation was detected at the β position. This suggests that a deuterium atom at the α position came from the *ortho* C–D bond of the substrate **1a-D**. The recovered starting material contained 0.72 H at the *ortho*-position, again indicating that the cleavage of the *ortho* C–H bond is reversible. A deuterium atom was also incorporated only at the α position in the reaction between **1a-D** and ethyl acrylate (Scheme 2d). The recovered starting material was also found to contain 0.52 H after the reaction. This result is similar to that observed in the case of the reaction with styrene, as shown in Scheme 2c.

To collect additional mechanistic information regarding this alkylation, a deuterated substrate bearing a free *ND* bond (**1a-ND**) was reacted with ethyl acrylate in the presence of deuterated acid PivOD (Scheme 3a). In sharp contrast to the *NH* substrate, such as **1a** and **1a-D**, a deuterium atom was incorporated at the β position (1.60 H), suggesting that a deuterium atom is transferred from a nitrogen to the β position. However, the ratio of the deuterium incorporation was not so high because *ND* is easily converted into *NH* in the presence of the acid additive (the deuterated acid can be converted into the protic acid form through reversible *ortho* C–H activation of the substrate). When the deuterated substrate **1a-D** was reacted in the absence of an alkene coupling partner for 8 h, H/D exchange was observed at the *ortho*-position (Scheme 3b). Thus, C–H activation is a reversible pathway.

We also carried out a kinetic isotope effect (KIE) study by conducting two individual experiments containing **1a** and the deuterated substrate **1a-D** with styrene (Fig. 1). The k_H/k_D ratio from these experiments was found to be 1.02, which further supports the conclusion that the C–H activation step is not the rate determining one.⁸

Based on the deuterium labelling experiments, the following plausible catalytic cycle is proposed (Scheme 4). Both catalysts $[\text{Rh}(\text{OAc})(\text{cod})]_2$ and $\text{Rh}_2(\text{OAc})_4$ were active for this transformation. The oxidative addition of an N–H bond to a Rh center provides Rh(III) or Rh(IV)^o species **A** (see ESI for details[†]) (the evidence of Rh(IV) formation was that the solution turned to a dark purple colour).¹⁰ In the next step, the insertion of an



Scheme 4 Proposed catalytic cycle.

alkene into the Rh–H bond gives intermediate **B**, in which the *NH* hydrogen is transferred to the β position, as evidenced by deuterium labelling experiments (Scheme 3a). Two possible pathways are proposed from intermediate **B**. The activation of the *ortho* C–H bond generates intermediate **D** *via* a CMD mechanism (path a) or the elimination of the carboxylic acid (path b), which involves the α -elimination of the carboxylic acid to form a carbene intermediate **C**.^{3i,m,11} The final step for path b involves the migratory insertion of the *ortho* C–H bond into the carbene in **C** to afford **D**. Fast deuterium scrambling occurred at the *ortho* C–H bond, hence ruling out the possibility that C–H activation is the rate determining step. In fact, the k_H/k_D ratio was 1.02. Subsequently, in the presence of carboxylic acid, reductive elimination takes place from **D** which results in the formation of the product along with the regeneration of the $[\text{Rh}]$ species which further continues the catalytic cycle. The most important result in the deuterium labelling experiments involved the finding that the *ortho* C–H bond is transferred only to the α -position of the product (Scheme 2c and d). If the reaction proceeded *via* path a, the *ortho* C–H bond would not be transferred to the product because it is eliminated as a carboxylic acid as a result of a CMD mechanism. Thus, path b is the most likely mechanism, however path a cannot be excluded completely.

Conclusions

In summary, we report herein the C–H alkylation of benzylamine derivatives catalysed by both Rh(I) and Rh(II) catalysts. A picolinamide derivative as the directing group for this transformation was found to be crucial for the reaction to proceed. The reaction has a broad substrate scope for the alkenes being used including α,β -unsaturated compounds and styrene derivatives and various substituted benzylamines were well tolerated.



To our delight, not only benzylamine but also other heterocycles such as a thiophene derived amine were also found to be suitable for the alkylation. The further novel applicability of this strategy involved the fact that the reaction is amenable to use under flow conditions. C–H activation chemistry under flow conditions is still a challenging and attractive field of research. Thus, our successful design of a flow set up for this alkylation process signifies its further scope and advantages. Mechanistic investigations suggest the possible involvement of a carbene mechanism for the reaction. Further expanding the scope of substrates for alkylation and other useful reactions under flow conditions is currently underway in our laboratory.

Conflicts of interest

There are no conflicts to declare.

Acknowledgements

This work was supported by a Grant in Aid for Specially Promoted Research by MEXT (No. 17H06091).

Notes and references

- (a) Z. Zhang and D. B. McCormick, *Proc. Natl. Acad. Sci. U. S. A.*, 1991, **88**, 10407–10410; (b) S. Maignan, J.-P. Guilloteau, S. Pouzieux, Y. M. Choi-sledeski, M. R. Becker, S. I. Klein, W. R. Ewing, H. W. Pauls, A. P. Spada and V. Mikol, *J. Med. Chem.*, 2000, **43**, 3226–3232; (c) R. Kolhatkar, C. D. Cook, S. K. Ghorai, J. Deschamps, P. M. Beardsley, M. E. A. Reith and A. K. Dutta, *J. Med. Chem.*, 2004, **47**, 5101–5113; (d) K.-J. Xiao, L. Chu, G. Chen and J.-Q. Yu, *J. Am. Chem. Soc.*, 2016, **138**, 7796–7800; (e) Z. Jiang, W. D. Hong, X. Cui, H. Gao, P. Wu, Y. Chen, D. Shen, Y. Yang, B. Zhang, M. J. Taylor, S. A. Ward, P. M. O'Neill, S. Zhao and K. Zhang, *RSC Adv.*, 2017, **7**, 52227–52237; (f) N. Mibu, K. Yokomizo, M. Sano, Y. Kawaguchi, K. Morimoto, S. Shimomura, R. Sato, N. Hiraga, A. Matsunaga, J. Zhou, T. Ohata, H. Aki and K. Sumoto, *Chem. Pharm. Bull.*, 2018, **66**, 830–838; (g) Y. Li, W. Yao, J. Lin, F. Li, Y. Wu and J. Xu, *J. Heterocycl. Chem.*, 2019, **56**, 2170–2178.
- For selected examples of C–H functionalizations of benzylamine derivatives, see: (a) K. Orito, A. Horibata, T. Nakamura, H. Ushito, H. Nagasaki, M. Yuguchi, S. Yamashita and M. Tokuda, *J. Am. Chem. Soc.*, 2004, **126**, 14342–14343; (b) G. Cai, Y. Fu, Y. Li, X. Wan and Z. Shi, *J. Am. Chem. Soc.*, 2007, **129**, 7666–7673; (c) Y. Zhao and G. Chen, *Org. Lett.*, 2011, **13**, 4850–4853; (d) M. Miura, C.-G. Feng, S. Ma and J.-Q. Yu, *Org. Lett.*, 2013, **15**, 5258–5261; (e) C. Lu, S.-Y. Zhang, G. He, W. A. Nack and G. Chen, *Tetrahedron*, 2014, **70**, 4197–4202; (f) Á. M. Martínez, J. Echavarren, I. Alonso, N. Rodríguez, R. Gómez-Arrayás and J. C. Carretero, *Chem. Sci.*, 2015, **6**, 5802–5814; (g) B. N. Laforteza, K. S. L. Chan and J.-Q. Yu, *Angew. Chem., Int. Ed.*, 2015, **127**, 11295–11298; (h) V. G. Landge, S. P. Midya, J. Rana, D. R. Shinde and E. Balaraman, *Org. Lett.*, 2016, **18**, 5252–5255; (i) Á. M. Martínez, N. Rodríguez, R. Gómez-Arrayás and J. C. Carretero, *Chem.-Eur. J.*, 2017, **23**, 11669–11676; (j) C. Kuai, L. Wang, B. Li, Z. Yang and X. Cui, *Org. Lett.*, 2017, **19**, 2102–2105; (k) U. Karmakar and R. Samanta, *J. Org. Chem.*, 2019, **84**, 2850–2861; (l) C. Dai, Y. Han, L. Liu, Z.-B. Huang, D.-Q. Shi and Y. Zhao, *Org. Chem. Front.*, 2020, **7**, 1703–1708.
- For reviews on C–H alkylations with alkenes, see: (a) Z. Dong, Z. Ren, S. J. Thompson, Y. Xu and G. Dong, *Chem. Rev.*, 2017, **117**, 9333–9403; (b) N. Chatani, *Bull. Chem. Soc. Jpn.*, 2018, **91**, 211–222. For selected examples from our group, see: (c) Y. Aihara and N. Chatani, *J. Am. Chem. Soc.*, 2013, **135**, 5308–5311; (d) G. Rouquet and N. Chatani, *Chem. Sci.*, 2013, **4**, 2201–2208; (e) K. Shibata and N. Chatani, *Org. Lett.*, 2014, **16**, 5148–5151; (f) K. Shibata, T. Yamaguchi and N. Chatani, *Org. Lett.*, 2015, **17**, 3584–3587; (g) Y. Aihara, J. Wuelbern and N. Chatani, *Bull. Chem. Soc. Jpn.*, 2015, **88**, 438–446; (h) Q. He, T. Yamaguchi and N. Chatani, *Org. Lett.*, 2017, **19**, 4544–4547; (i) K. Shibata, S. Natsui, M. Tobisu, Y. Fukumoto and N. Chatani, *Nat. Commun.*, 2017, **8**, 1448; (j) S. Rej and N. Chatani, *ACS Catal.*, 2018, **8**, 6699–6706; (k) Q. He and N. Chatani, *J. Org. Chem.*, 2018, **83**, 13587–13594; (l) S. Rej and N. Chatani, *Chem. Commun.*, 2019, **55**, 10503–10506; (m) T. Yamaguchi, S. Natsui, K. Shibata, K. Yamazaki, S. Rej and Y. Ano, *Chem.-Eur. J.*, 2019, **25**, 6915–6919; (n) C. Wang, S. Rej and N. Chatani, *Chem. Lett.*, 2019, **48**, 1185–1187; (o) N. Ohara, S. Rej and N. Chatani, *Chem. Lett.*, 2020, **49**, 1053–1057.
- (a) B. Gutmann, D. Cantillo and C. O. Kappe, *Angew. Chem., Int. Ed.*, 2015, **54**, 6688–6728; (b) S. A. May, *J. Flow Chem.*, 2017, **7**, 137–145; (c) D. Dallinger and C. O. Kappe, *Curr. Opin. Green Sustain. Chem.*, 2017, **7**, 6–12; (d) A. R. Bogdan and A. W. Dombrowski, *J. Med. Chem.*, 2019, **62**, 6422–6468; (e) M. Baumann, T. S. Moody, M. Smyth and S. Wharry, *Org. Process Res. Dev.*, 2020, **24**(10), 1802–1813.
- For a book chapter, see: (a) T. F. Jamison and G. Koch, *Science of Synthesis: Flow Chemistry in Organic Synthesis*, 1st edn, Georg Thieme Verlag KG: Stuttgart, 2018. DOI: 10.1055/b-006-161272. For recent reviews, see: (b) D. Webb and T. F. Jamison, *Chem. Sci.*, 2010, **1**, 675–680; (c) R. Porta, M. Benaglia and A. Puglisi, *Org. Process Res. Dev.*, 2016, **20**, 2–25; (d) M. B. Plutschack, B. Pieber, K. Gilmore and P. H. Seeberger, *Chem. Rev.*, 2017, **117**, 11796–11893; (e) S. Santoro, F. Ferlin, L. Ackermann and L. Vaccaro, *Chem. Soc. Rev.*, 2019, **48**, 2767–2782; (f) S. Govaerts, A. Nyuchev and T. Noël, *J. Flow Chem.*, 2020, **10**, 13–71. For selected examples, see: (g) M. Christakakou, M. Schön, M. Schnürch and M. D. Mihovilovic, *Synlett*, 2013, **24**, 2411–2418; (h) H. P. L. Gemoets, G. Laudadio, K. Verstraete, V. Hessel and T. Noël, *Angew. Chem., Int. Ed.*, 2017, **56**, 7161–7165; (i) G. Laudadio, S. Govaerts, Y. Wang, D. Ravelli, H. F. Koolman, M. Fagnoni, S. W. Djuric and T. Noël, *Angew. Chem., Int. Ed.*, 2018, **57**, 4078–4082; (j) X. Wei, I. Abdiaj, C. Sambiagio, C. Li, E. Zysman-colman, J. Alcázar and T. Noël, *Angew. Chem., Int. Ed.*, 2019, **58**, 13030–13034; (k) G. Laudadio, Y. Deng, K. Van Der Wal, D. Ravelli, M. Nuño, M. Fagnoni, D. Guthrie, Y. Sun and



T. Noël, *Science*, 2020, **369**, 92–96; (l) Z. Wen, A. Maheshwari, C. Sambiagio, Y. Deng, G. Laudadio, K. V. Aken, Y. Sun, H. P. L. Gemoets and T. Noël, *Org. Process Res. Dev.*, 2020, **24**, 2356–2361.

6 (a) H. P. L. Gemoets, V. Hessel and T. Noël, *Org. Lett.*, 2014, **16**, 5800–5803; (b) J. Zakrzewski, A. P. Smalley, M. A. Kabeshov, M. J. Gaunt and A. A. Lapkin, *Angew. Chem., Int. Ed.*, 2016, **55**, 8878–8883; (c) H. Wang, F. Pesciaioli, J. C. A. Oliveira, S. Warratz and L. Ackermann, *Angew. Chem., Int. Ed.*, 2017, **56**, 15063–15067; (d) U. K. Sharma, H. P. L. Gemoets, F. Schröder, T. Noël and E. V. Van der Eycken, *ACS Catal.*, 2017, **7**, 3818–3823; (e) F. Ferlin, S. Santoro, L. Ackermann and L. Vaccaro, *Green Chem.*, 2017, **19**, 2510–2514; (f) F. Ferlin, L. Luciani, S. Santoro, A. Marrocchi, D. Lanari, A. Bechtoldt, L. Ackermann and L. Vaccaro, *Green Chem.*, 2018, **20**, 2888–2893; (g) C. Zhu, J. C. A. Oliveira, Z. Shen, H. Huang and L. Ackermann, *ACS Catal.*, 2018, **8**, 4402–4407; (h) A. Bouchard, V. Kairouz, M. Manneveau, H. Xiong, T. Basset, X. Panneccoucke and H. Lebel, *J. Flow Chem.*, 2019, **9**, 9–12; (i) W.-J. Kong, L. H. Finger, A. M. Messinis, R. Kuniyil, J. C. A. Oliveira and L. Ackermann, *J. Am. Chem. Soc.*, 2019, **141**, 17198–17206.

7 (a) T. W. Lyons and M. S. Sanford, *Chem. Rev.*, 2010, **110**, 1147–1169; (b) M. Zhang, Y. Zhang, X. Jie, H. Zhao, G. Li and W. Su, *Org. Chem. Front.*, 2014, **1**, 843–895; (c) Z. Chen, B. Wang, J. Zhang, W. Yu, Z. Liu and Y. Zhang, *Org. Chem. Front.*, 2015, **2**, 1107–1295; (d) C. Sambiagio, D. Schönbauer, R. Blieck, T. Dao-Huy, G. Pototschnig, P. Schaaf, T. Wiesinger, M. F. Zia, J. Wencel-Delord, T. Basset, B. U. W. Maes and M. Schnürch, *Chem. Soc. Rev.*, 2018, **47**, 6603–6743; (e) P. Gandeepan and L. Ackermann, *Chem.*, 2018, **4**, 199–222; (f) S. Rej, Y. Ano and N. Chatani, *Chem. Rev.*, 2020, **120**, 1788–1887; (g) J. I. Higham and J. A. Bull, *Org. Biomol. Chem.*, 2020, **18**, 7291–7315.

8 (a) M. Gómez-Gallego and M. A. Sierra, *Chem. Rev.*, 2011, **111**, 4857–4963; (b) Y. Xia, Z. Liu, S. Feng, Y. Zhang and J. Wang, *J. Org. Chem.*, 2015, **80**, 223–236.

9 S. B. Sinha, D. Y. Shopov, L. S. Sharninghausen, D. J. Vinyard, B. Q. Mercado, G. W. Brudvig and R. H. Crabtree, *J. Am. Chem. Soc.*, 2015, **137**, 15692–15695.

10 (a) S. A. Macgregor, *Organometallics*, 2001, **20**, 1860–1874; (b) J. Zhao, A. S. Goldman and J. F. Hartwig, *Science*, 2005, **307**, 1080–1083; (c) I. Mena, M. A. Casado, P. García-Orduña, V. Polo, F. J. Lahoz, A. Fazal and L. A. Oro, *Angew. Chem., Int. Ed.*, 2011, **50**, 11735–11738; (d) E. Vélez, M. P. Betoré, M. A. Casado and V. Polo, *Organometallics*, 2015, **34**, 3959–3966.

11 (a) N. D. Jones, G. Lin, R. A. Gossage, R. McDonald and R. G. Cavell, *Organometallics*, 2003, **22**, 2832–2841; (b) T. Cantat, M. Demange, N. Mezailles, L. Ricard, Y. Jean and P. Le Floch, *Organometallics*, 2005, **24**, 4838–4841; (c) H. Heuclin, X. F. Le Goff and N. Mezailles, *Chem.-Eur. J.*, 2012, **18**, 16136–16144; (d) F. Hu, Y. Xia, C. Ma, Z. Yan and J. Wang, *Chem. Commun.*, 2015, **51**, 7986–7995.

